Available online at www.sciencedirect.com

ScienceDirect

Procedia Engineering 4 (2010) 145–152

Procedia Engineering

www.elsevier.com/locate/procedia

ISAB-2010

Multi-mode vortex-induced vibration of slender cable experiencing shear flow

Weimin Chen[a,]*, Zhongqin Zheng[a], Min Li[b]

[a]*Key Laboratory of Environmental Mechanics, Institute of Mechanics, CAS, Beijing 100190, China*
[b] *School of Aeronautics Sciences and Engineering, Beijing University of Aeronautics and Astronautics, Beijing 100191, China*

Received 13 July 2010; revised 25 July 2010; accepted 30 July 2010

Abstract

The dynamic characteristics of slender cable often present serried modes with low frequencies due to large structure flexibility resulted from high aspect ratio (ratio of length to diameter of cable), while the flow velocity distributes non-uniformly along the cable span actually in practical engineering. Therefore, the prediction of the vertex-induce vibration of slender cable suffered from multi-mode and high-mode motions becomes a challenging problem. In this paper a prediction approach based on modal energy is developed to deal with multi-mode lock-in. Then it is applied to the modified wake-oscillator model to predict the VIV displacement and stress responses of cable in non-uniform flow field. At last, illustrative examples are given of which the VIV response of flexible cable in nonlinear shear flow field is analyzed. The effects of flow velocity on VIV are explored. Our results show that both displacement and stress responses become larger as the flow velocity increasing; especially higher stress response companied with higher frequency vibration should be paid enough attention in practical design of SFT because of its remarkable influence on structure fatigue life.

Keywords: vortex-induced vibration; mode; internal wave; shear flow; wake-oscillator

1. Introduction

For a vibrating cable experiencing non-uniform flow, the wake field, body motion and the coupling between fluid and structure are more complex than the case of uniform flow, e.g. the vortex mode and shedding frequency vary along the cable length, or no longer maintain constant. Moreover, the dynamic characteristics of slender cable tend to reveal low-frequency and high-density natural modes due to large flexibility. Therefore the vortex-induce vibration (VIV) of a slender cable experiencing non-uniform flow may present some new phenomena such as multi-mode lock-in [1–6] , travelling wave and wide–band random vibration. Its response prediction becomes more complex.

* Corresponding author. Tel.: +86-10-82543891; fax: +86-10-82338527.
E-mail address: wmchen@imech.ac.cn

doi:10.1016/j.proeng.2010.08.017

Some large-scale experiments and 3D CFD simulations have been implemented in recent years. The vortex mode and fluid force distribution for lower Re numbers (mainly for Re=10^2-10^3) are presented by numerical simulations. While mechanism analysis and empirical formula based on large-scale experiments has been developed. Among these researches [7–13] the multi-mode vibration and drag coefficient given by Huarte [6], high-mode (10-25) lock-in by Vandiver [12] and modal analysis of experimental results by Huse [7] and Lie [13] provided fruitful base for analysis of multi-mode VIV.

In this paper a novel prediction approach of multi-mode VIV is developed. Based on the modal energy, the locked mode as well as its original modal weight is identified from potential vibration modes. Then the modal parameter such as the lock-in length, effective mass and damping can be calculated. Consequently the final response is given by employing the modified wake oscillator model. A satisfactory agreement between the response of the presented approach and the results of large-scale experiments is observed. Moreover, the approach benefiting from its convenient and fast calculation is suitable for application to practical engineering. At last, illustrative examples are given of which the effect of flow distribution on the VIV of cable is discussed.

2. Basic model

2.1. Multi-mode lock-in in shear flow

When the flow velocity varies along the cable span, it is observed experimentally that the wake vortex sheds from the cable in the manner of vortex cells where the shedding frequency keeps constant in one cell and jumps discontinuously from one cell to another. When the lock-in occurs, the shedding frequency in a cell is consistent with a certain natural frequency of the cable, and the cell number depends on the span distribution of flow velocity and the dynamic characteristics of structure. Note that in different cells the vortex may shed at different frequencies. In this sense, multiple natural modes may be excited and each mode has its lock-in span region among which exciting vibration energy is applied to structure by the ambient fluid and beyond which structure vibration energy is damped along the cable by the ambient fluid.

The natural frequency of potential locked modes should fall into range of $f_{lock}^{\min} \le f_n \le f_{lock}^{\max}$ according the Strouhal law, where $f_{lock}^{\min} = S_t V_{\min} / D$, $f_{lock}^{\max} = S_t V_{\max} / D$, $V_{\min}$ and $V_{\max}$ are the minimum and maximum values of the flow velocity respectively, f_n is the frequency of the n th mode, D is the diameter of cable. Further, the position and length L_n of modal lock-in region can be determined by the value of reduced velocity $V_r = V / f_n D$ (V is the flow velocity) satisfying $4 \le V_r \le 12$ and the span distribution of flow velocity. However troubles are raised in that large variety of modes (even beyond 20) may simultaneously resonance and the lock-in region may overlap or even interlace. In fact it was experimentally indicated that the number of locked mode is really limited (around 10). Additionally, the number and order of the locked mode may be different from that of experiments sometimes, if the rule of higher-order-mode priority is used by which the higher-order mode is always prior over the lower-order mode in vibration.

In this paper, we introduce a parameter describing the modal energy as the level of the original weight so as to identify the locked mode from large variety of potential exciting modes and subsequently to determine lock-in region. The potential modal energy is expressed in terms of the power of the exciting mode as follows,

$$P_n = (F_n)^2 / (2R_n) \tag{1}$$

where the modal force $F_n = \int_{L_n} (1/2) C_L \rho V(z)^2 D(z) \varphi_n^2(z) dz$ and the modal damping $R_n = R_{hn} + R_{sn}$. z is the coordinate in span-wise direction, L_n is the exciting length of mode n, $\varphi_n(z)$ is the mode shape, ρ is the fluid density, C_L is the vortex-induced lift coefficient and usually takes a value of 0.8 [12] for a flexible cable; R_{hn} and R_{sn} are the modal hydrodynamic damping and structural damping respectively.

The modal structure damping $R_{sn} = 2\xi_{Sn} M_n \omega_n$, M_n is the modal mass and $\omega_n = 2\pi f_n$. Generally, modal hydrodynamic damping is much greater than structural damping and written as [12]

$$R_{hn} = \int_{L-L_n} r_h(z)\varphi_n^2(z)\omega_n dz \tag{2}$$

where L is the total length of cable. At lower reduced velocity the hydrodynamic damping $r_h(z)$ is $r_h(z) = r_{sw} + C_{rl}\rho DV$, where the static damping $r_{sw} = \dfrac{\omega\pi\rho D^2}{2}\left(\dfrac{2\sqrt{2}}{\mathrm{Re}_\omega} + C_{sw}\right)$, $\mathrm{Re}_\omega = \omega D^2/\upsilon$, υ is viscous of fluid, C_{sw} and C_{rl} are constant and have values of 0.2 and 0.06 respectively. While at higher reduced velocity we have $r_h(z) = C_{rh}\rho V^2/\omega$. The constant C_{rh} is 0.2. Hence the modal damping can be written as

$$R_n = \int_{L-L_n} r_h(z)\varphi_n^2(z)\omega_n dz + \int_L r_s(z)\varphi_n^2(z)\omega_n dz \tag{3}$$

It should be pointed out that only those of powerful mode rather than all of potential modes are finally locked because of the interaction and competition between the potential vibrating modes. So the dimensionless modal energy $\overline{P}_n = P_n/(P_n)_{\max}$ is taken to indicate the competition level of mode n, where $(P_n)_{\max}$ is the maximum value of P_n. And the mode satisfying $\overline{P}_n \geq 0.10$ is finally regarded as a locked mode.

2.2. VIV response of cable

The displacement and stress response of locked modes and the final response of cable are calculated by the modified wake oscillator model [3, 15] that considers the variation of added mass and the non-linear relationship between reduced velocity and displacement amplitude, and is particularly suitable for VIV of flexible cable in non-uniform flow. The effective mass [3, 15] of mode n is written as

$$v_n = \frac{\int_0^L m(z)\varphi_n^2(z)dz}{\int_0^L s(z)\varphi_n^2(z)dz} \tag{4}$$

where $m(z)$ is the structure mass of unit length, $s(z)$ is the lock-in index having a value of 1.0 in lock-in region and a value of 0.0 in non-lock-in region. The displacement amplitude is $Y_n(z) = DF_n I_n^{-1/2}\varphi(z)$ where the shape coefficient $I_n = \int_0^L m(z)\varphi_n^4(z)dx \Big/ \int_0^L m(z)\varphi_n^2(z)dx$ and F_n is the amplified coefficient. The damping ratio ζ_n^S of the system and the amplified coefficient F_n can be obtained by a iteration calculation according to the formula $F_n = 1/[1+9.6(\mu_r^n\zeta_n^s)^{1.8}]$, where the modal mass ratio $\mu_r^n = v_n/m_D$, m_D is the displaced mass. Let $\zeta_n^S = \zeta_n^I + F_n\phi_n$, then the effective damping of mode n is written as

$$\phi_n = \frac{2D\int_0^L C_D(z)\rho D[1-s(z)]\left|\varphi_n(z)\right|^3 dz}{3\pi[\int_0^L m\varphi_n^4(z)dz]^{1/2}[\int_0^L m\varphi_n^2(z)dz]^{1/2}} \tag{5}$$

where the drag coefficient is generally taken as a constant $C_D = 1.2$. Total response of the cable is the summation of all locked modes, i.e. $Y(z) = \sum_n Y_n(z) = \sum_n w_n \varphi_n(z)$, where w_n is the final modal weight of the n th locked mode and its non-dimensional form is $\overline{w}_n = w_n / (w_n)_{\max}$, $(w_n)_{\max}$ is the maximum value of w_n.

2.3. Verification of the model

In order to verify the presented model, the VIV response of a slender cable experiencing linear shear flow is calculated and compared with the experimental results [7]. The parameters of the cable are listed in Table 1. The modal weights and the displacement response at 0.54m/s and 1.14m/s flow velocity are plotted in Fig. 1 and Fig. 2 respectively and listed in Table 2.

In Fig. 1(a) both the priority mode, mode 11, and the locked modes, modes 8-20, are consistent with the experimental results except an additional one, mode 3 of the calculation. For case of experiment those modes below the 8th were cut-off, or only the modes between 8-30 were included in the modal analysis. However the displacement response including mode 3, either the RMS average value in Table 2 or the RMS distributions in Fig. 1(b), are closer to the experimental results in comparison to the response excluding mode 3. Further, since the addition of the 3rd mode as well as its weight on the final response, the modal weights of mode 12, 13 and 14 are less than experimental values, as presented in Fig. 1(a). Compared with the calculation by the previous wake oscillator model [16] the displacement RMS agrees better with the experimental curve as shown in Fig. 1(b), and the previous model presented a different priority mode, the 13th mode [16] from the experimental results.

Table 1. Parameters of the cable (unit: m/s/kg)

Length	Inner/outer diameter	Youngs modulus	Density	Top tension
90	0.026/0.03	2.1×10^{11}	3211	3700

Table 2. VIV response of the cable (unit: m/s/kg)

	0.54m/s velocity			1.14m/s velocity		
	RMS average	Priority mode	Locked modes	RMS average	Priority mode	Locked modes
Calculations	7.21	11	3, 8-20	8.60	22	10-25
	6.83	11	8-20			
Experiments	7.35	11	8-20	7.47	22,15	10-25
Ref. [21]	6.83	13				

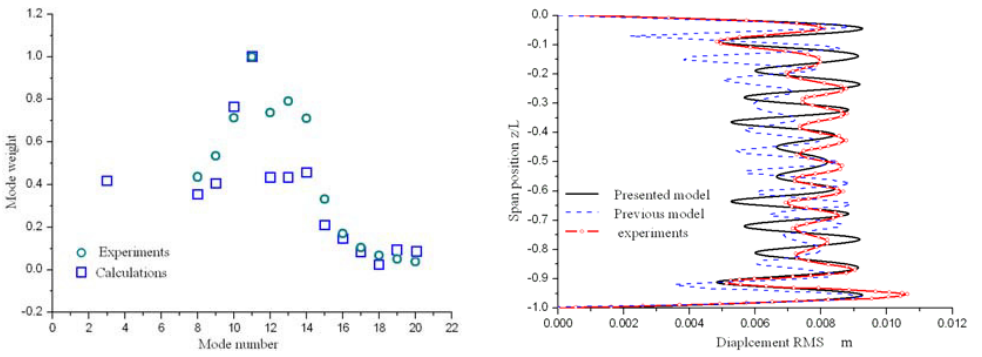

(a) (b)

Fig. 1. VIV response at 0.54m/s flow velocity: (a) Modal weights $\overline{w}_n$; (b) Displacement RMS distribution

For case of 1.14m/s flow velocity, both the locked modes, 10-25, and the priority mode, 22, are consistent with that of experiments, as shown in Fig. 2(a) and Table 2. The displacement RMS in Fig. 2(b) among the exciting regime (0-0.40 cable span) generally agrees with the experimental curve, whereas the vibration keeps the same level rather than the experimental attenuation as approaching the cable bottom due to the travelling effect. Hence the average value of the calculated displacement RMS based on standing wave assumption is 15.1% greater than the experimental value.

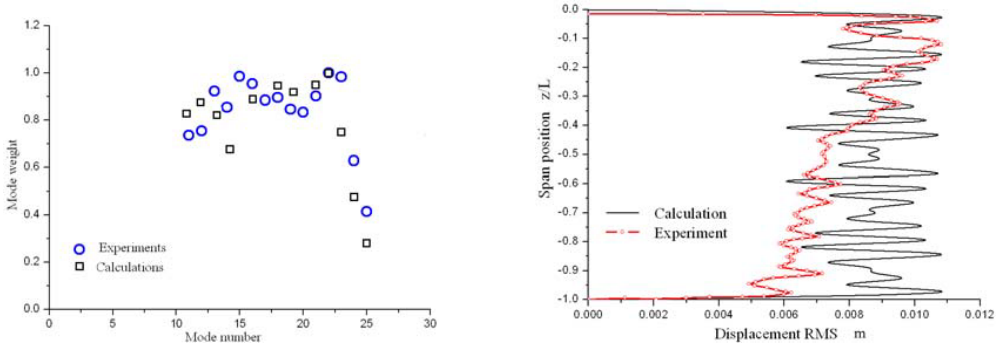

(a) (b)

Fig. 2. VIV response at 1.14m/s flow velocity: (a) Modal weights of locked modes; (b) Displacement RMS distribution

3. Applications and discussion

3.1. VIV response of slender cable in nonlinear shear flow

The parameters of a slender cable attached by buoyancy rings with 1.4m diameter are: 0.53m and 0.425m outer and inner diameters respectively, 3000m length, 582kg/m^3 density, 2.10E+11 Youngs modulus and 3.20E+07 N top tension. Two nonlinear shear flow profiles, the velocity and distribution span length of Flow 1 are respectively half of and double of that of the Flow 2, are shown in Fig. 3. The natural frequencies and the corresponding Strouhal velocity $V_{St}^n = f_n D / S_t$ are shown in Fig. 4 where $S_t = 0.17$ [14] for a flexible cable, rather than $S_t = 0.20$ for a rigid cylinder. The responses of dimensionless displacement Y/D and stress $\sigma/\sigma_{\max}$ ($\sigma_{\max} = 2.35\times10^6$/Pa) are presented in Table 3 and Fig. 5. Compared with the Flow 1, the Flow 2 has smaller span length with higher flow velocity as well as larger modal exciting length (0.10-0.50 cable span). So the effective mass and damping (Eq. (4) and (5)) of the system in the Flow 2 are smaller and consequently the final response becomes larger, as shown in Fig. 5.

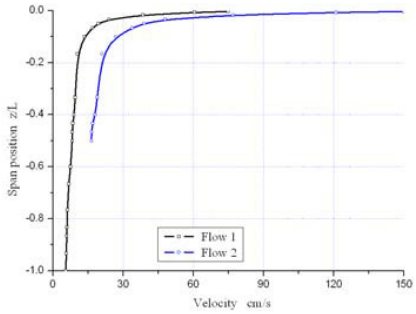

Fig. 3. Flow velocity profile

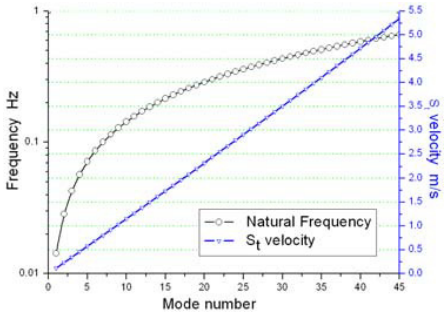

Fig. 4. The natural frequencies of structure and the St velocities versus the mode number

Table 3. Averaged response of the cable undergoing two flows

	Flow 1	Flow 2
Locked modes	1-6	1-12
Averaged displacement RMS	0.08	0.26
Displacement amplitude average	0.14	0.28
Averaged stress RMS	0.43	0.82
Stress amplitude average	0.52	1.00

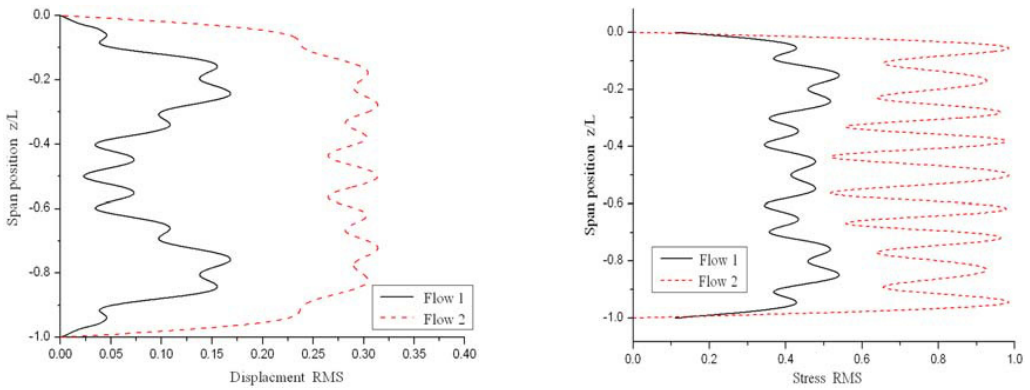

Fig. 5. Response of cable undergoing non-uniform flows: (a) Displacement RMS distribution; (b) Stress RMS distribution

3.2. Effect of flow velocity on VIV response

The average values of the displacement and stress RMS undergoing the Flow 1 are plotted against the maximum flow velocity in Fig. 6, while the flow profile along the cable span is proportionally maintained. The displacement RMS in Fig. 6(a) tends to increase as the flow velocity becoming larger except at some flow velocities, e.g. V=0.8, 1.8 and 2.0m/s. And there exist two response regimes, i.e. around 0.08-0.15 displacement RMS at flow velocity ranging from 0.4 to 1.0m/s and then jumping up around 0.30-0.45 displacement RMS at 1.2-3.0m/s flow velocity.

The displacement jumping may be due to a significant increase of the exciting length resulted from new locked modes along 0.50-1.00 cable span as the flow velocity increasing.

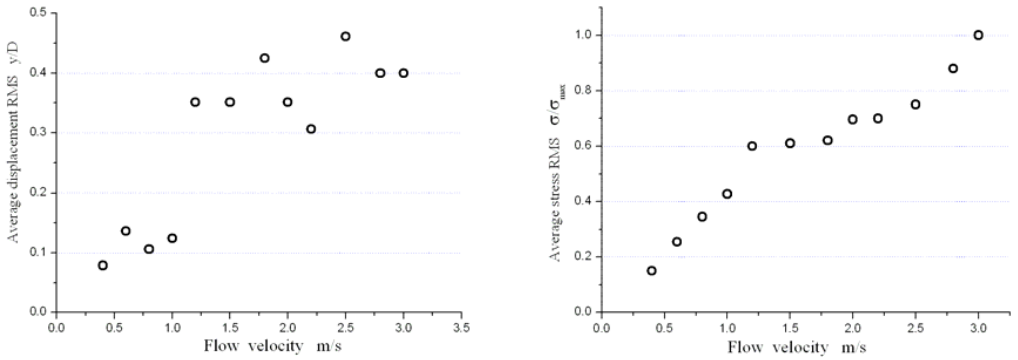

(a) (b)

Fig. 6. VIV response versus flow velocity: (a) Average displacement RMS versus flow velocity; (b) Average stress RMS versus flow velocity

Fig. 6(b) indicates that stress RMS increases monotonically as the flow velocity becoming larger. Because successive higher order modes are excited as flow velocity monotonically increasing, that has larger deformation curvature and higher modal stress. Moreover, higher stress responses are generally companied with higher frequency vibration, that should be noted in practical design of SFT because of its remarkable influence on structure fatigue life.

4. Conclusions

An approach based on modal energy is developed here to solve the problem mainly raised from multi-mode lock-in. It is applied to the modified wake-oscillator model to predict the VIV displacement and stress response of slender cable. Illustrative examples are given, by which the VIV analysis of flexible cable in linear and nonlinear shear flow fields is carried out. Effect of flow velocity on VIV is explored. Our results show that:

(1) Compared with case of the Flow 1, the cable in Flow 2 has larger modal exciting regimes. So the effective mass and damping of the system are smaller and consequently the final response in the Flow 2 is larger.

(2) Displacement RMS tends to increase as the flow velocity becoming larger except at some flow velocities. And there exist two response regimes due to a significant increase of the exciting length resulted from new locked modes along 0.50-1.00 cable span as the flow velocity increasing.

(3) Stress RMS increases monotonically as the flow velocity becoming larger. Because successive higher order modes are excited as flow velocity increasing, that has larger deformation curvature and higher modal stress. Moreover, higher stress responses are generally companied with higher frequency vibration, which should be paid enough attention in practical design of SFT because of its remarkable influence on structure fatigue life.

Acknowledgements

This work is financially supported by the Knowledge Innovation Program of the Chinese Academy of Sciences (no. KJCX2-YW-L07) and the National Natural Science Foundation of China (no. 10772183).

References

[1] Lyons GJ, Patel MH. A prediction technique for vortex induced transverse response of marine risers and tethers. *Journal of Sound and Vibration* 1986; 111 (3): 467–87.

[2] Chen WM, Wang Y. Effects of tension and flow distribution on the vortex-induced vibration of TLP tethers. *Shipbuilding of China* 2004; 45sp: 226–31. (in Chinese)

[3] Chen WM, Zhang LW, Li M. Prediction of vortex-induced vibration of flexible riser using an improved wake-oscillator model. *Proceedings of the ASME 28th International Conference on Ocean, Offshore and Arctic Engineering*, Honolulu, Hawaii, 2009.

[4] Lyons G J, Patel MH. A prediction technique for vortex induced transverse response of marine risers and tethers. *Journal of Sound and Vibration* 1986; 111 (3): 467–87.

[5] Ge F, Hui L, Hong Y. vortex-induced vibration of submarine floating tunnel undergoing shear flow. *Journal of the Graduate School of the Chinese Academy of Sciences* 2007; 24(3): 352–6. (in Chinese)

[6] Bokaian A. Lock-in prediction of marine risers and tethers. *Journal of Sound and Vibration* 1994; 175 (5): 607–23.

[7] Huera HF, Bearman PW, Chaplin JR. On the force distribution along the axis of a flexible circular cylinder undergoing multi-mode vortex-induced vibrations. *Journal of Fluids and Structures* 2006; 22: 897–903.

[8] Huse E, Kleiven G, Nielsen FG. Large scale model testing of deep sea risers. *Proceedings of the Offshore Technology Conference*, Houston, Texas, 1998, OTC 8701.

[9] Huse E, Kleiven G, Nielsen FG. VIV-induced axial vibration on deep sea risers. *Proceedings of the Offshore Technology Conference*, Houston, Texas, 1999, OTC 10932.

[10] Dong S, Karniadakis GE. DNS of flow past a stationary and oscillating cylinder at Re=10000. *Journal of Fluids and Structures* 2005; 20: 519–31

[11] Al-Jamal H, Dalton C. Vortex induced vibrations using large eddy simulation at a moderate Reynolds number. *Journal of Fluids and Structures* 2004; 19: 73–92

[12] Yamamoto CT, Meneghini JR, Saltara F. Numerical simulations of vortex-induced vibration on flexible cylinders. *Journal of Fluids and Structures* 2004; 19: 467–89.

[13] Vandiver JK. A universal reduced damping parameter for prediction of vortex-induced vibration. *Proceedings of the 20th International Conference on Offshore Mechanics and Arctic Engineering*, Oslo, Norway, 2002.

[14] Lie H, Kaasen HK. Modeal analysis of measurements from a large-scale VIV model test of a riser in linearly sheared flow. *Journal of Fluid and Structures* 2006; 22: 557–75.

[15] Wang Y, Chen WM, Lin M. Study on the variation of added mass and its application to the calculation of amplitude response for a circular cylinder at lock-in. *China Ocean Engineering* 2007, 21(3): 429–37.

[16] Xu WH, Zeng XH, Wu YX. High aspect ratio (L/D) riser VIV prediction using wake oscillator model. *Ocean Engineering* 2008; 35: 1769–74.